Draft version August 12, 2025
Typeset using LaTeX **twocolumn** style in AASTeX631

The Instrument and Sky: Best Birds
(but we're angry)

Liam Becker,[1] Sydney Pemble,[1] Ishaani Purang,[1] Tristen Arias,[1] and Jeffrey Lan[1]

[1] *University of Washington - ASTR 481*

ABSTRACT

Team Best Birds spent four nights operating the Manastash Ridge Observatory taking calibration images and observing standard field SA41-SF1 in B and V across a range of airmasses in the aim of characterizing and understanding the sky and CCD, Evora at MRO. In my analysis of Evora, I calculate the gain to be 1.59 e^- per ADU, read-noise to be 9.44 ADUs, and dark current to be an insignificant 7.47×10^{-3} ADUs per second. I find that Evora behaves linearly for exposures longer than 2 seconds and for exposures that do not exceed 55,000 ADUs. To standardize my photometry, I derive extinction coefficients of $k_B = 1.48$ and $k_V = 0.858$ and transformation coefficients of $\mu_{\rm B} = 0.0987$, $C_{\rm B} = 21.3$, $\mu_{\rm V} = -0.686$, and $C_{\rm V} = 21.9$; all reasonable values. When used to standardize our images of 26 Draconis, I calculate magnitudes of $B = 6.20$ and $V = 5.60$, roughly 0.4 magnitudes above the literature values.

1. INTRODUCTION

Our team observed at the Manastash Ridge Observatory (MRO), located in central Washington state (at a latitude of 46 57 03.95, longitude of longitude of -120 43 28.33, and altitude of 1198 m), every night from Thursday, July 3, 2025, to Sunday, July 6, 2025. The 30" telescope at MRO has a field of view (FOV) of 8 arcminutes by 8 arcminutes and its CCD (Charge-Coupled Device) has a plate scale of 0.98 arcseconds per pixel. It has six filters: the Johnson B and V filters, the Sloan g', r', and i' filters, and an H-alpha filter (Fraser 2025). Our aims in this trip were to characterize the linearity and dark current of the CCD, Evora, and to derive the extinction and transformation coefficients of the instrument and sky at MRO.

Table 1 details the observing conditions at the observatory during our four-night run; the weather was mostly favorable, but cloudy skies kept us from observing for the majority of the second night. It is also important to note that as the run progressed, the moon was more illuminated and set later, leading to much brighter skies in the final nights.

In Section 2, I characterize MRO's CCD, Evora, determining the gain, read-noise, and dark current in 2.1, before analyzing the linearity of Evora in 2.2. I detail our observations and my methods of reduction in Section 3, discuss my photometry in Section 4, determining the optimal aperture radius in 4.1. In Section 5, I derive extinction and transformation coefficients, correcting for atmospheric extinction in 5.1 and color standardization in 5.2, before applying the corrections to 26 Draconis in 5.3.

Night	Date	Weather	Seeing	Illum %	Moonset
1	07/03/25	clear-ish	7.0	64	01:04
2	07/04/25	cloudy	5.6	73	01:25
3	07/05/25	clear	3.9	81	01:46
4	07/06/25	clear	3.3	88	02:16

Table 1: Table of information regarding the weather, seeing, illumination percentage of the moon, and the time of moonset at MRO during the nights of our observations. The seeing was determined via the full width at half-maximum (FWHM) for the star directly to the right of 26 Draconis in the B-band fields we took each night—found with the Star tool on the Astroart application (Cavicchio & Nicolini 2025).

2. CCD CHARACTERIZATION

In order to understand how to process my data, the first step is understanding the properties of the 1024 x 1024-pixel CCD used for observations at MRO, Evora. In this section I walk through the steps I took to characterize the CCD and explain the decisions I made to correct for any effects Evora may have on my data.

Corresponding author: Liam Becker
liamb27@uw.edu

2.1. *Gain, Read-Noise, and Dark Current*

A CCD counts the photons it collects by measuring the voltage difference due to electrons kicked from the atoms of the chip via the photoelectric effect ("photoelectrons"). The electronics of the CCD convert this voltage into counts, or ADUs (Analog-to-Digital Units), which are recorded by each pixel during an exposure—the number of photoelectrons converted to a single ADU is called the gain of the CCD. To calculate the gain of Evora I used Eq. 1, where S is the mean signal from two flats and σ^2_Δ is found by the difference between the flats and taking the variance (Sánchez-Gallego 2025). With domeflats in the V filter, I calculated the gain to be 1.59 e^- per ADU.

$$G = 2\frac{S}{\sigma^2_\Delta} \tag{1}$$

The minimum signal a pixel must receive to be recorded is called the read-noise of a CCD. To calculate the read-noise of Evora I found the variance between two bias frames (σ^2_Δ) and plugged the value into Eq. 2, finding the read-noise to be 9.44 ADUs or 15.04 photoelectrons (Sánchez-Gallego 2025).

$$\sigma_{\rm RN} = \sqrt{\frac{\sigma^2_\Delta}{2}} \tag{2}$$

Another source of noise inherent to the CCD is that which comes from the thermal energy of the chip and is referred to as dark current noise. Since Evora is cooled to -88 °C, I didn't expect there to be much dark current, and the plot in Figure 1 shows this to be true. Using bias-subtracted dark exposures from 60 to 900 seconds, I fit a first-degree polynomial and find the dark current to be 7.47×10^{-3} ADUs per second, or 1.19×10^{-2} photoelectrons per second, with a baseline dark noise (y-intercept) of 25.7 ADUs or 40.9 photoelectrons. As I will explain in Section 3.2, I determined the dark current to be insignificant to my observations and chose not to correct for it in my reductions.

2.2. *Linearity of Evora*

Photometry relies on the linearity of a CCD—an increase in photons causes a proportional increase in signal, allowing the astronomer to calculate the flux of a target. An ideal CCD converts light intensity into voltage perfectly linearly, however, the reality isn't as exact; a CCD like Evora has two limits on its linearity: the capacity of its pixels and the speed of its shutter.

The pixels of a CCD can only hold a certain amount of charge, which in the case of Evora, is around 60,000 ADUs. Upon reaching this maximum, the electrons leak into nearby pixels, leaving trails of signal across the image that are undesirable when doing photometry. To avoid over-filling pixels during imaging, I took flats of increasing exposure time and plotted the bias-subtracted median value of the image in Figure 2a. The plot indicates a peak at roughly 60,000 ADUs, after which point the median value decreases. Before the peak, Evora is essentially linear, so I decided that for high-count exposures, pixels below 55,000 ADUs are linear and can be used for science.

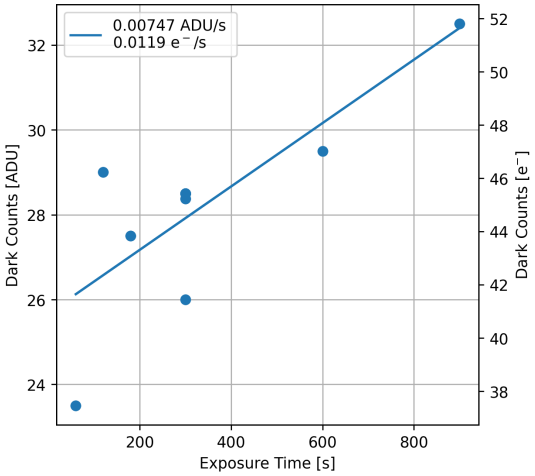

Figure 1: Plotted here are the counts for dark exposures from 60 to 900 seconds, fitted with a first-degree polynomial. The left y-axis shows the counts in ADUs and the right y-axis shows the counts in photoelectrons.

Typically, the time it takes for the shutter to open and close is insignificantly small compared to the exposure time, but when imaging bright sources, short exposure times may become comparable to the speed of the shutter so as not to overexpose the image. To determine the lower limit for exposures, I took flats of decreasing exposure time and plotted the bias-subtracted median values of each image in Figure 2b.

The plot seems to show that Evora maintains linearity down to exposures as short as 0.01 seconds, but inspecting these images reveals a clear shutter pattern, shown by the darker areas in Figure 3. Inspecting these shorter exposures, I decided not to take any science images with exposure times shorter than 2 seconds in order to avoid the signature of the shutter.

3. OBSERVATIONS & METHODS

3.1. *Observations*

In order to accurately standardize the observations made at MRO, we observed the standard field SA41-SF1 (hereby referred to as SF1) from Landolt (2013), which contains stars ranging from $B - V = +0.246$ to

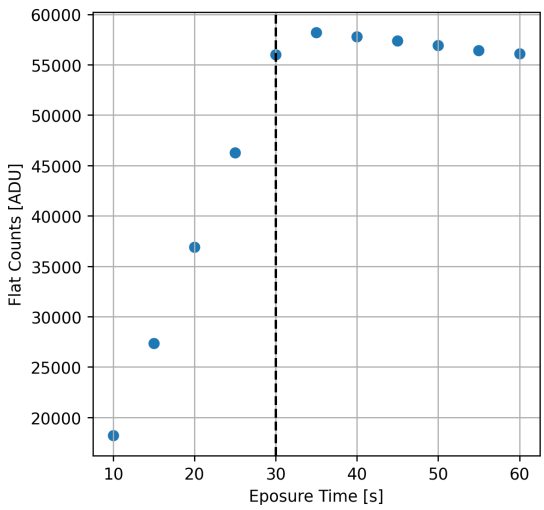

(a) High-count linearity test

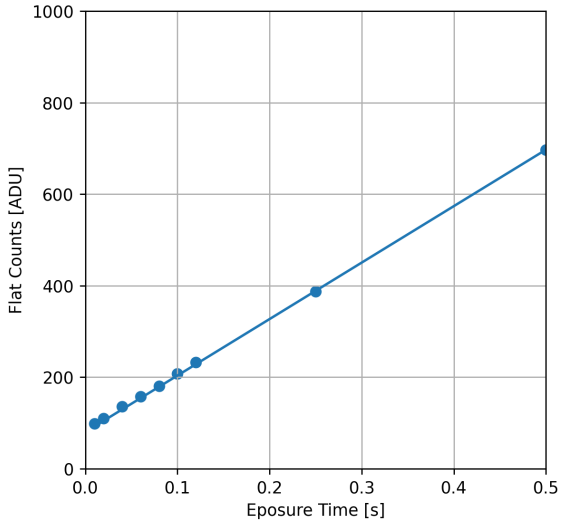

(b) Low-exposure time linearity test

Figure 2: Plots showing the linearity of Evora across a wide range of exposure times. Panel (a) shows that Evora loses its linearity around 55,000 ADUs, while panel (b) seems to demonstrate no significant degradation in linearity in exposures as low as 0.01 seconds.

+1.320, listed in Table 2 along with 26 Draconis, our target star, upon which I perform the standardizations discussed in Section 5.

Over the course of a night we took images of SF1 at varying altitudes, and thus, varying airmasses to measure the effect of atmospheric extinction at MRO. Every star in SF1 is dimmer than 13th magnitude and required exposures of 300 to 600 seconds in order to get sufficient signal to noise. As stars traverse higher airmasses,

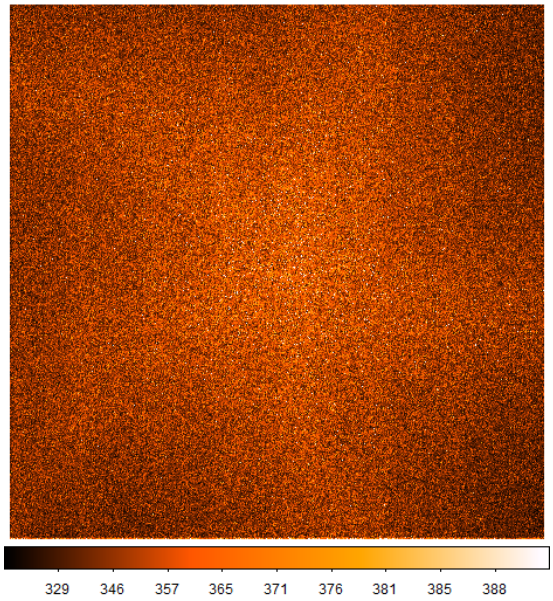

Figure 3: This 0.01-second flat shows the shadow cast by Evora's shutter onto the CCD.

the airmass value changes more rapidly compared to the lower airmasses near zenith; this, along with our long exposures, caused significant gaps in airmass between our low-altitude observations that may cause errors when correcting for atmospheric extinction. We attempted to image SF1 on all four nights of our observing run, but were only able to effectively gather extinction data on nights three and four.

OBJECT	RA	DEC	V	(B-V)
SA 41-620	21 53 11.306	+45 36 21.13	14.176	+0.770
SA 41-626	21 53 17.263	+45 37 24.48	14.058	+0.911
SA 41-625	21 53 17.295	+45 35 14.74	14.205	+0.876
SA 41-631	21 53 24.561	+45 35 45.09	13.390	+0.246
SA 41-634	21 53 27.209	+45 35 40.95	13.164	+0.738
SA 41-637	21 53 30.416	+45 36 11.04	14.426	+1.199
SA 41-638	21 53 32.591	+45 37 00.50	14.045	+0.736
SA 41-639	21 53 33.743	+45 34 20.95	14.130	+1.320
26 Dra	17 34 59.624	+61 52 28.241	5.21	+0.595

Table 2: Table of details for our standard field (*top eight rows*) and target star (*bottom row*). Data for the extinction stars come from Table 2 in Landolt (2013), and data for the target star come from SIMBAD, which cites Fabricius et al. (2002).

I initially intended to exclusively use data collected on night four, which had the best seeing, however, I believe issues in the telescope's tracking caused the stars in our standard field to appear elliptical rather than circular.

My struggles with night four's images drove me to reduce and analyze the data we collected on night three instead.

3.2. *Removing the Instrumental Signature*

Before analyzing the data we took during our observing run, I had to remove the instrumental signature and reduce the images. This process entailed bias subtraction, analysis of the dark current, creation of an illumination correction, and the application of these calibrations to the science images.

I noticed that the bias files differ between the nights of observation, so I used sigma-clipping to create a median bias for each night. When creating my median flats and reducing my science images I made sure to use the bias file from the corresponding night in order to correct for any unique signatures that may exist in the biases for each night.

As mentioned in Section 2.1, the dark current of Evora is very low and contributes roughly 30 counts for our 600-second science exposures. I find this contribution to be insignificant compared to the thousands of ADUs of signal from our stars, so I chose not to subtract the dark frames from my images to avoid contributing more noise to the reduction.

Unfortunately, we started our observations too late to get skyflats on night three, so I used those collected during night two for my reduction. There were cloudy skies during night two, which provided a star-less flat field—the telescope was sufficiently unfocused and multiple flats were averaged such that no structure is visible in the normalized master skyflat. Additionally, the only night we took domeflats was night four, which I used to determine the gain in Section 2.1.

Using my code from ASTR 480, I subtracted the bias from my flats, took the median combination, and normalized the skyflats and domeflats separately. To smooth my median skyflat into an illumination correction, I used `Gaussian2DKernel` from `astropy` with a standard deviation of 20 pixels, shown in Figure 4b (Astropy Collaboration et al. 2022). The median skyflat I used (Figure 4a) exhibits the "dust donuts" typical of a domeflat, due to the high signal to noise ratio present in the skyflats we took (on the order of 100). The median skyflat contains both low-frequency (illumination pattern) and high-frequency (dust donuts) noise, so I chose to only use the skyflat in the reduction of my images, rather than the illumination correction or domeflats.

To reduce the science images, I subtracted the bias and divided by the median skyflat. I also applied `astroscrappy.detect_cosmics` to remove any cosmic rays. The raw and reduced images of our standard field are shown in Figure 5.

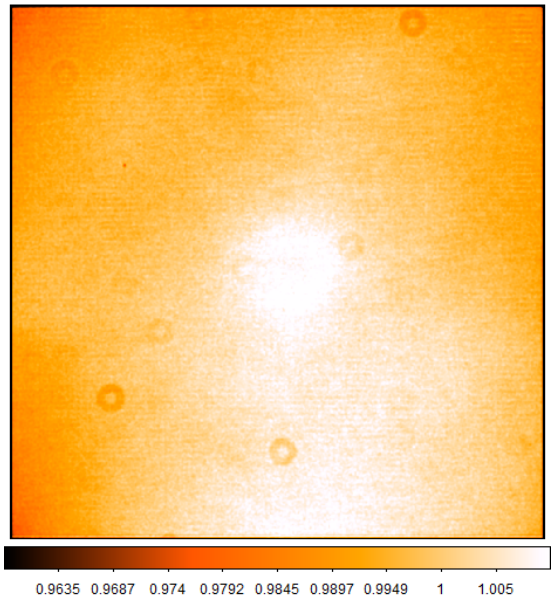

(a) Bias-subtracted median skyflat in V

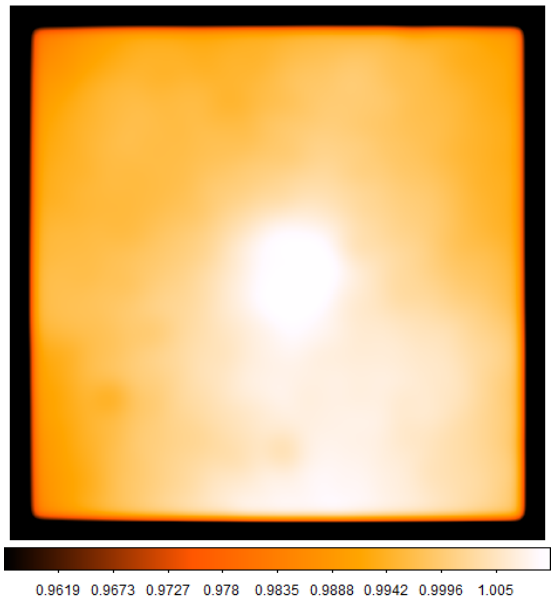

(b) Illumination correction in V

Figure 4: Shown here are (a) the median skyflat in V from night two and (b) the illumination correction created from the skyflat using `astropy`'s `Gaussian2DKernel` with a 20 pixel standard deviation (Astropy Collaboration et al. 2022). The signal from the skyflat was high enough such that "dust donuts" are visible in the image. The dark border on the illumination correction appears to be an artifact from the smoothing.

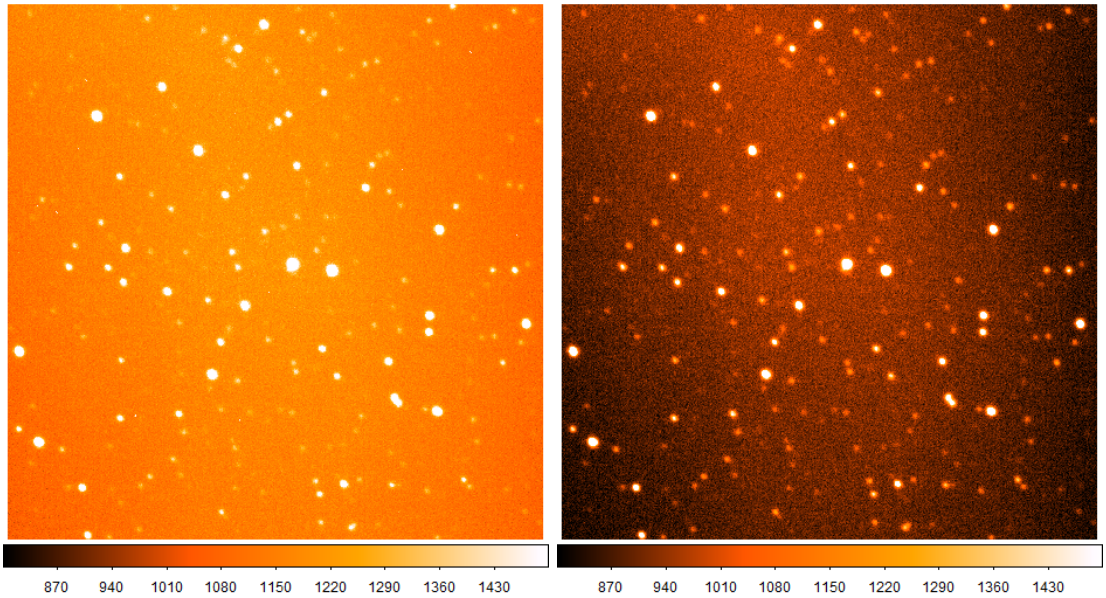

Figure 5: Pictured here are the raw *(left)* and reduced *(right)* images of our standard field SA41 SF1 (Fig. 76 in Landolt (2013)). This was a 600-second exposure at an airmass of 1.028 in the V filter.

4. PHOTOMETRY

With my images reduced, I used `photutils` to do the photometry, using the `DAOStarFinder` function to determine the centroids of the stars (Bradley et al. 2024). The FOV of the 30-inch at MRO is 8' x 8', which doesn't cover the entire 15' x 15' field of SF1 from Landolt (2013), so I chose to analyze only the stars listed in Table 2.

4.1. *Determining Aperture Radius*

The optimal radius for aperture photometry is that which maximizes the signal to noise ratio (SNR). To do this, I performed aperture photometry for each of the eight stars in SF1 at many radii, calculated the SNR with the CCD Equation, Eq. 3, and plotted the SNR for each star at each radius, shown in Figure 7 alongside the instrumental magnitude calculated for each aperture.

$$S/N = \frac{gN_*}{\sqrt{gN_* + n_{\rm pix} gN_{\rm sky} + n_{\rm pix}\sigma_{\rm RN}^2}} \tag{3}$$

The CCD Equation calculates the SNR of an aperture from the gain (g), number of counts collected by the aperture in ADUs (N_*), number of pixels in the circular annulus used for the photometry ($n_{\rm pix}$), number of counts collected by the annulus in ADUs ($N_{\rm sky}$), and the read-noise calculated in Section 2.1 ($\sigma_{\rm RN}$).

By averaging the maximum of each SNR curve, I found the "Best Radius" (BR) to take my photometry data from, roughly 5.60 pixels—smaller than the $\sim$ 7.5-pixel FWHM, determined with Astroart (Cavicchio & Nicolini 2025). This radius, plotted over SF1 in Figure 6, only excludes around 0.31 magnitudes of the total flux of each star, which I determined by averaging the difference between the flux at the largest radius and the flux at the BR. In my photometry tables, I correct for this excluded flux before further analysis.

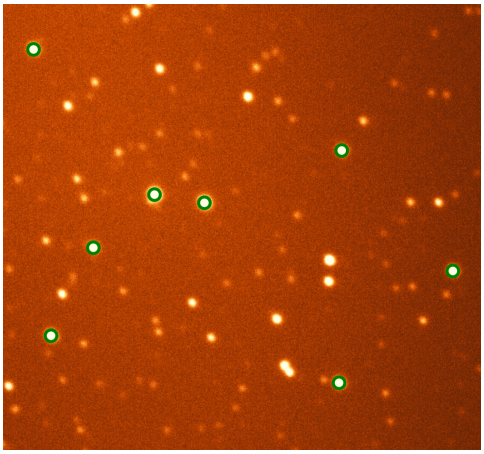

Figure 6: SF1, cropped with the BR-apertures plotted in green on the eight stars.

5. EXTINCTION & TRANSFORMATION COEFFICIENTS

5.1. *Atmospheric Extinction*

With photometry done for each of the eight stars in SF1 across a wide range of airmasses, I plotted the instrumental magnitudes (b & v) vs. airmass (X) and fit Eq. 4 to the data to determine the extinction coefficients (k_B & k_V), shown in Figure 8. Taking the median values

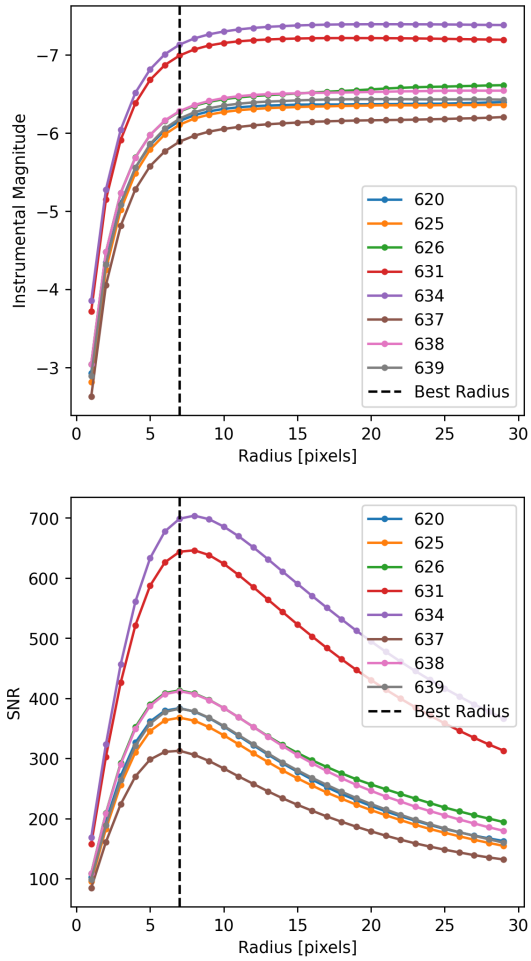

Figure 7: Plotted here are the results of aperture photometry at radii from 1 to 30 pixels for the eight stars in SF1 at an airmass of 1.028 in the V filter. *Top:* Instrumental magnitude vs. aperture radius, where it is clear that very little signal is omitted by the "Best Radius" (BR); *Bottom:* SNR vs. aperture radius, with the BR determined by averaging the maximum location of each star's SNR curve.

of k across each star in SF1 for each filter, I calculate the extinction coefficients to be $k_B = 1.48$ and $k_V = 0.858$.

$$\begin{aligned} b &= b_0 + k_B X \\ v &= v_0 + k_V X \end{aligned} \tag{4}$$

Both coefficients are positive, correctly demonstrating that magnitude *increases* with airmass; light is absorbed and scattered by the atmosphere, so stars appear dimmer when observed through more of it. Interestingly, k_B is greater than k_V by nearly a factor of two, implying atmospheric extinction is correlated to wavelength—something seen every day in the sky's blue hue as the atmosphere scatters shorter-wavelength light more than longer-wavelength light.

With the extinction coefficients for each filter, I use Eq. 4 to solve for b_0 and v_0, the extinction-corrected instrumental magnitudes for my stars. This quantity represents the instrumental magnitude of the star, were it observed without any atmosphere, or "above the atmosphere" and without the associated extinction.

5.2. *Color Standardization*

The final step in standardizing photometry is color standardization—CCDs are sensitive to different colors to different degrees, so it is necessary to correct for the color-dependence to accurately measure the magnitude of a star. To find my color correction coefficients I took $(B - b_0)$ and $(V - v_0)$, the standard magnitudes in B or V from Landolt (2013) minus the extinction-corrected instrumental magnitudes I calculated in Section 5.1 and plotted it against $(b_0 - v_0)$, the extinction-corrected magnitudes for B minus those for V, shown in Figure 9.

$$\begin{aligned} (B - b_0) &= \mu_B (b_0 - v_0) + C_B \\ (V - v_0) &= \mu_V (b_0 - v_0) + C_V \end{aligned} \tag{5}$$

To these data I fit a first-degree polynomial to determine μ and C in Eq. 5, which I find to be $\mu_{\mathrm{B}} = 0.0987$, $C_{\mathrm{B}} = 21.3$, $\mu_{\mathrm{V}} = -0.686$, and $C_{\mathrm{V}} = 21.9$. These coefficients indicate that Evora is roughly half of a magnitude more sensitive in V than B and within each filter, slightly more sensitive to *bluer* stars (low B-V) in the B filter and slightly more sensitive to *redder* stars (high B-V) in the V filter. These trends seem to diverge, perchance indicating a minimum sensitivity between the B and V filters, but the slopes are very small and their divergence may be simply a result of random error.

5.3. *Application*

With the extinction and transformation coefficients of the observatory determined, I performed aperture photometry (with BR= 12.5 pixels) on B and V images of our target star, 26 Dra, using Eq. 4 to correct the effect of 1.028 airmass and Eq. 5 to standardize its magnitude. The results of the process are listed in Table 3, where my values of $B = 6.20$ and $V = 5.60$ are compared to the literature values of 5.80 and 5.21, respectively (Fabricius et al. 2002).

The results I got are fairly close but both estimate a brightness roughly 0.4 magnitudes too dim, compared to the accepted values. Seeing as these values differ by the same amount, I would predict the error lies in C or k, not μ, since the star has the same $(b_0 - v_0)$ value in both filters and the result would not be affected by the slopes in Figure 9.

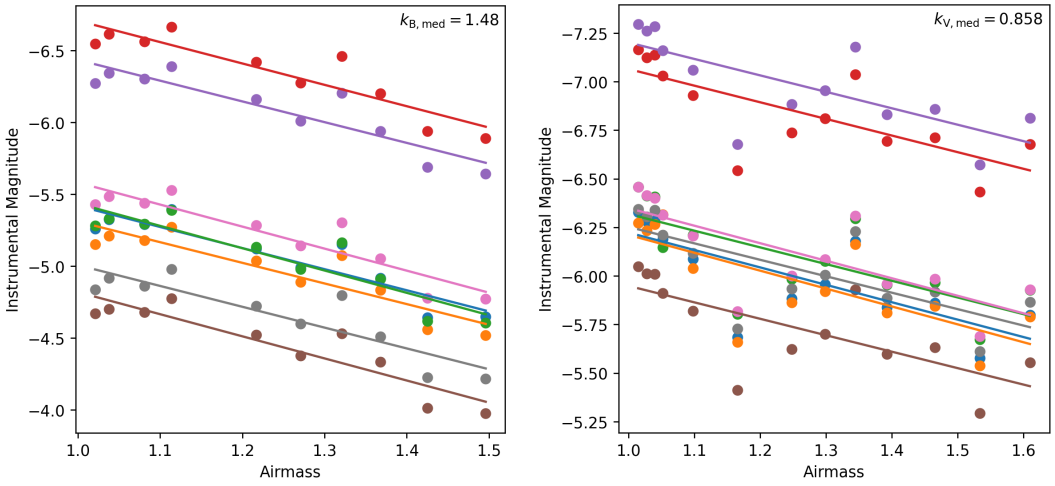

Figure 8: Instrumental magnitude plotted as a function of airmass for the stars in SF1 in B (*left*) and V (*right*). Each star is fitted with a first-degree polynomial and the median of the slopes (extinction coefficients) for each filter is shown in the top right corner of each panel.

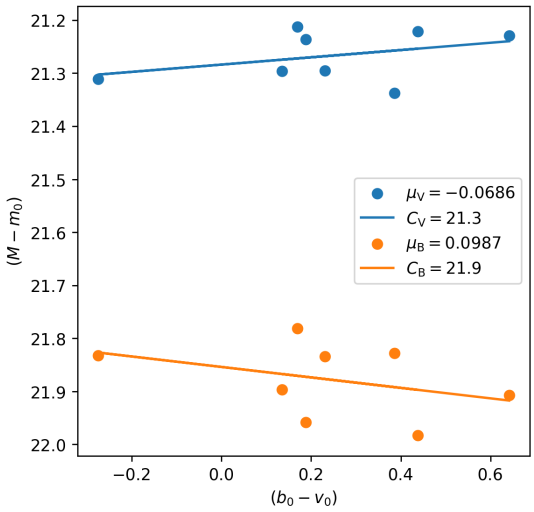

Figure 9: Standard magnitude minus extinction-corrected instrumental magnitude plotted vs. instrumental B-V. Data for V is plotted in blue (*top*) and for B in orange (*bottom*). Transformation coefficients for each filter are listed in the legend.

b	v	b_0	v_0	B	V	B_*	V_*
-14.13	-14.79	-15.71	-15.70	6.20	5.60	5.80	5.21

Table 3: Table of B and V magnitudes for 26 Dra throughout the standardization process. From left to right, the sections are raw instrumental magnitude, extinction-corrected instrumental magnitude, color-standardized magnitude, and literature magnitudes from SIMBAD, which cites Fabricius et al. (2002).

The most likely source of error I can imagine is the airmass values used to determine k; since our exposures were 10 minutes long, SF1 moved significantly across the sky and the airmass changed over the course of the exposure, meaning the airmass recorded at the start of the exposure differed from the airmass at the end by several hundredths, in some cases. Unfortunately, we only captured two non-overexposed images of 26 Dra on night two—one in B and one in V—so I don't have the data to see if the error changes with airmass.

6. SUMMARY

Across the four nights that Team Best Birds operated the Manastash Ridge Observatory, we took many calibration and science images, observing standard field SA41-SF1 from Landolt (2013) in the B and V filters across a range of airmasses. From these data I used biases, darks, and flats to determine the gain (1.59 e^- per ADU), read-noise (9.44 ADUs), dark current (7.47×10^{-3} ADUs per second), and linearity range (2 seconds of exposure, up to ~55,000 ADUs) of the CCD, Evora. I ultimately chose not to perform a dark correction in my reduction, seeing as the dark current was so low. Additionally, I decided not to use the illumination correction I created, given the high-SNR skyflats we took.

I used the biases and skyflats to reduce our images of SF1 from night two, found the "Best Radius" for aperture photometry by maximizing the SNR, and used Eq. 4 to determine the extinction coefficients: $k_B = 1.48$ and $k_V = 0.858$. With the extinction-corrected magnitudes, I used Eq. 5 to fit the transformation coefficients, $\mu_B = 0.0987$, $C_B = 21.3$, $\mu_V = -0.686$, and $C_V = 21.9$.

Finally, I applied the extinction and transformation coefficients to images of 26 Draconis, taken in B and V, to standardize my photometry of the star. The magnitudes I calculated are $B = 6.20$ and $V = 5.60$, which are both roughly 0.4 magnitudes above the literature values, indicating a largely successful standardization.

ACKNOWLEDGMENTS

Special thanks to Team Best Birds for making our trip to MRO so enjoyable; to Tristen Arias for having good time-management and being there to compare results, and to Ishaani Purang for sticking with me through our droughts of brain-function as we both did our best to finish this report. Thank you to Professor Oliver Fraser for your continued leniency with deadlines that allowed me to submit the best work I'm capable of. Thank you to Devanshi Singh for guilt-tripping me to get out of my apartment and actually do work. Finally, shout-out to the dumbbell that hit me in the forehead, that was super cool and awesome and fun!

REFERENCES

Astropy Collaboration, Price-Whelan, A. M., Lim, P. L., et al. 2022, ApJ, 935, 167, doi: 10.3847/1538-4357/ac7c74

Bradley, L., Sipőcz, B., Robitaille, T., et al. 2024, astropy/photutils: 2.0.2, 2.0.2, Zenodo, doi: 10.5281/zenodo.13989456

Cavicchio, F., & Nicolini, M. 2025, Astroart, MSB Software. https://msb-astroart.com/default.htm

Fabricius, C., Høg, E., Makarov, V. V., et al. 2002, A&A, 384, 180, doi: 10.1051/0004-6361:20011822

Fraser, O. 2025, University of Washington. https://uwmro.github.io/

Landolt, A. U. 2013, AJ, 146, 131, doi: 10.1088/0004-6256/146/5/131

Sánchez-Gallego, J. 2025, Basic CCD reductions. https://uw-astro-480.github.io/lecture_notes/ccd_reductions/ccd_reductions.html